High-Pressure Phase Behavior of Ionic Liquid/CO$_2$ Systems

Lynnette A. Blanchard, Zhiyong Gu, and Joan F. Brennecke*

Department of Chemical Engineering, University of Notre Dame, Notre Dame, Indiana 46556

Received: September 16, 2000; In Final Form: January 9, 2001

This work presents the high-pressure phase behavior of CO$_2$ with six ionic liquids: 1-*n*-butyl-3-methylimidazolium hexafluorophosphate ([bmim][PF$_6$]), 1-*n*-octyl-3-methylimidazolium hexafluorophosphate ([C$_8$-mim][PF$_6$]), 1-*n*-octyl-3-methylimidazolium tetrafluoroborate ([C$_8$-mim][BF$_4$]), 1-*n*-butyl-3-methylimidazolium nitrate ([bmim][NO$_3$]), 1-ethyl-3-methylimidazolium ethyl sulfate ([emim][EtSO$_4$]), and *N*-butylpyridinium tetrafluoroborate ([*N*-bupy][BF$_4$]). We explored the effect of systematically changing the anionic and cationic components of the ionic liquid on the CO$_2$−ionic liquid phase behavior. For all of the ionic liquids tested, large quantities of CO$_2$ dissolved in the ionic liquid phase, but no appreciable amount of ionic liquid solubilized in the CO$_2$ phase. In addition, the liquid phase volume expansion with the introduction of even large amounts of CO$_2$ is negligible, in dramatic contrast to the large volume expansion observed for neutral organic liquids. Our results seek to elucidate the underlying physical mechanisms of this highly unusual phase behavior.

Introduction

Ionic liquids (ILs), a novel class of organic solvents, have been the focus of much research in recent years. ILs are organic salts composed of cations and anions that are liquid at conditions around room temperature.[1] Although there are many classes of salts that can have melting points near ambient temperature (e.g., alkylammonium and phosphonium salts), two important groups of ILs are those based on imidazolium and pyridinium cations.[2,3] Many compounds of these two classes have melting points at or below room temperature. Early investigations used mainly chloroaluminate-based ionic liquids that are unstable in the presence of water. A dramatic growth in the development of ILs has eliminated this hydroscopic liability with the synthesis of water-stable and even water-miscible ionic liquids, making their use as solvents much more feasible.[4] ILs have proven to be viable reaction media for numerous types of reactions, including, for example, Friedel−Crafts alkylations and Diels−Alder reactions.[5] Ionic liquids have a notable advantage over traditional organic solvents: vanishingly small vapor pressures. The importance of this lies in the potential to utilize ILs as solvents in traditional processes in efforts to eliminate the large volume of fugitive emissions typical of volatile organic solvents.

While the focus of research on ILs has predominantly been on their applicability as solvents for reaction systems, investigation and development of separation methods is equally essential and relatively unexplored. Several techniques for solute recovery from ionic liquids exist. Distillation (or evaporation), a reasonable option owing to the lack of any appreciable IL vapor pressure, would not be prudent for thermally labile or low-volatility products. ILs exhibiting immiscibility with water can be exploited by means of liquid−liquid extraction in efforts to separate solutes from the IL into the aqueous phase. For example, recent work has developed a reversible pH-dependent liquid−liquid partitioning of a solute between an ionic liquid phase and an aqueous phase.[6] While successful, the important

factor of cross-contamination between the phases presents a problem. Also, the partitioning of the solute between the phases limits the extent of solute extraction.[7] Another option, supercritical fluid extraction with CO$_2$, was first introduced by the quantitative extraction of naphthalene from 1-*n*-butyl-3-methylimidazolium hexafluorophosphate ([bmim][PF$_6$]).[8] Subsequent work has shown that a wide variety of solutes can be extracted from [bmim][PF$_6$] with CO$_2$ with recovery rates greater than 95%.[9] It should be noted that all solutes were recovered without any IL contamination. Thus, the problem of cross-contamination is eliminated since the IL does not appreciably solubilize in the CO$_2$ phase and depressurization completely removes CO$_2$ from the IL phase.

Preliminary work has shown supercritical CO$_2$ extraction to be a viable method for solute recovery from an IL; however, knowledge of the phase behavior of the CO$_2$−IL systems is a crucial aspect of this methodology. The first preliminary investigation of IL−CO$_2$ phase behavior indicated that these are very unusual biphasic systems. Although large quantities of CO$_2$ dissolved in the IL-rich phase, reducing the IL viscosity, no measurable amount of [bmim][PF$_6$] solubilized in the CO$_2$-rich phase. The system remained two distinct phases, even under pressures up to 400 bar.[8] It is the truly unique phase behavior [bmim][PF$_6$] has with CO$_2$, high-pressure phase behavior unlike any normal organic liquid/CO$_2$ system,[10] that makes the extraction of solutes from an IL with CO$_2$ particularly attractive.

The focus of this work is to develop insights into the physical interactions between CO$_2$ and ionic liquids that yield this interesting phase behavior. Here we present the results of a fundamental study that explores the phase behavior of CO$_2$ with a variety of different imidazolium- and pyridinium-based ILs:

[bmim][PF$_6$], 1-*n*-butyl-3-methylimidazolium hexafluorophosphate;

[C$_8$-mim][PF$_6$], 1-*n*-octyl-3-methylimidazolium hexafluorophosphate;

[C$_8$-mim][BF$_4$], 1-*n*-octyl-3-methylimidazolium tetrafluoroborate;

[bmim][NO$_3$], 1-*n*-butyl-3-methylimidazolium nitrate;

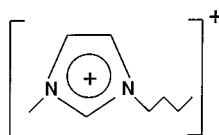* Corresponding author: phone (219) 631-5847; fax (219) 631-8366; e-mail jfb@nd.edu.

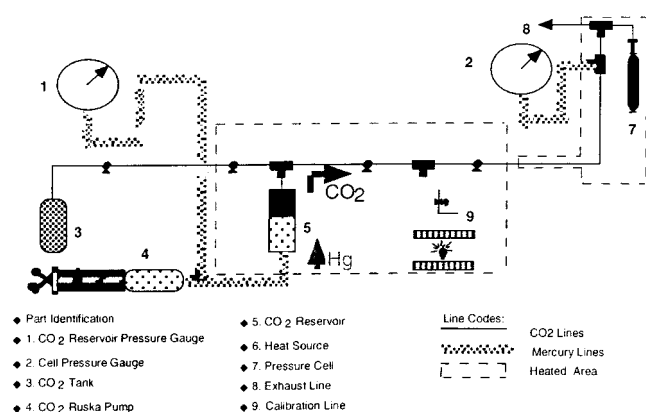**Figure 1.** Schematic of the structure of [bmim][PF$_6$].

Part Identification		Line Codes:
◆ 1. CO$_2$ Reservoir Pressure Gauge	◆ 5. CO$_2$ Reservoir	CO2 Lines
◆ 2. Cell Pressure Gauge	◆ 6. Heat Source	Mercury Lines
◆ 3. CO$_2$ Tank	◆ 7. Pressure Cell	Heated Area
◆ 4. CO$_2$ Ruska Pump	◆ 8. Exhaust Line	
	◆ 9. Calibration Line	

Figure 2. Static high-pressure vapor−liquid equilibrium apparatus.

[emim][EtSO$_4$], 1-ethyl-3-methylimidazolium ethyl sulfate; and

[*N*-bupy][BF$_4$], *N*-butylpyridinium tetrafluoroborate.

Phase behavior of CO$_2$ with 1-methylimidazole, a nonionic organic liquid used in the synthesis of the imidazolium-based ILs, was also measured to provide a nonionic organic compound for comparison.

Experimental Section

All ionic liquids were dried and degassed under vacuum at room temperature for several days prior to use. Measurements in our laboratory and others have shown that [bmim][PF$_6$], for example, will absorb a couple weight percent of water when left open to the atmosphere. The estimated water content of [bmim][PF$_6$] after drying was approximately 0.15 wt % water, as measured by Karl Fischer analysis. [bmim][PF$_6$], 1-*n*-butyl-3-methylimidazolium hexafluorophosphate, was obtained from Sachem. The chemical structure for [bmim][PF$_6$] is given in Figure 1. The following samples were synthesized by Seddon and co-workers at The Queen's University of Belfast:

[C$_8$mim][PF$_6$], 1-*n*-octyl-3-methylimidazolium hexafluorophosphate;

[C$_8$mim][BF$_4$], 1-*n*-octyl-3-methylimidazolium tetrafluoroborate;

[bmim][NO$_3$], 1-*n*-butyl-3-methylimidazolium nitrate;

[*N*-bupy][BF$_4$], *N*-butylpyridinium tetrafluoroborate; and

[emim][EtSO$_4$], 1-ethyl-3-methylimidazolium ethyl sulfate.

1-Methylimidazole, 99% purity, was used as received from Aldrich. Carbon Dioxide, anaerobic grade, 99.99% purity, was obtained from Mittler Gas Supply.

High-pressure vapor−liquid phase behavior was measured with two different apparatuses: a static high-pressure phase equilibrium system and a dynamic flow apparatus. The solubility of CO$_2$ in the IL-rich phase was measured at 40.0, 50.0, and 60 ± 0.1 °C, for each IL sample, with the static equilibrium apparatus shown in Figure 2.[11,12] The maximum pressure accessible with this apparatus is 120 bar. A glass cell was loaded with approximately 1.0 g of the IL sample and placed in a constant-temperature bath. Known amounts of CO$_2$ were metered into the glass cell while the sample within was vigorously stirred to ensure equilibrium. The composition of
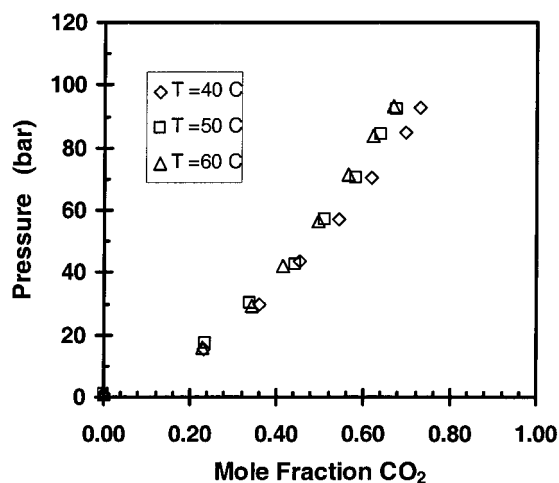

Figure 3. [bmim][PF$_6$]−CO$_2$ liquid phase compositions at 40, 50, and 60 °C.

the IL-rich liquid phase was calculated on the basis of the known amount of CO$_2$ added to the cell, along with the assumption of a pure CO$_2$ vapor phase. This assumption was verified by experiments on the dynamic apparatus. CO$_2$ was completely removed from the IL phase upon depressurization. The estimated uncertainties in the calculated liquid phase compositions and liquid molar volumes are ±0.002 mole fraction and ±0.2 mL/mol, respectively, based on propagation of random errors in the measurements of the temperatures, pressures and volumes.

The dynamic apparatus, an ISCO 220SX high-pressure extractor, was used to measure the solubility of the IL in the CO$_2$-rich phase. A sample cartridge, loaded with a small sample of the IL and glass beads, was pressurized with CO$_2$ at 40 ± 1 °C and 137.9 ± 0.2 bar. The saturated CO$_2$ phase was depressurized through a heated restrictor and collected in a flask of ethanol, which was analyzed by UV−visible spectroscopy. All of the ILs studied have strong absorbances in the UV−vis.

In addition, pure component density measurements were performed at three temperatures, 40 ± 1, 50 ± 1, and 60 ± 1 °C, for each ionic liquid at ambient pressure (0.98 ± 0.03 bar). The ionic liquid was loaded into a pycnometer of known volume and submerged in a constant-temperature bath. Upon thermal equilibrium, the amount of IL in the pycnometer was determined gravimetrically. The estimated uncertainty of the density measurements at ambient pressure is ±0.007 g/mL.

Results

[bmim][PF$_6$]−CO$_2$. The solubility of CO$_2$ in [bmim][PF$_6$] was determined at 40, 50, and 60 °C and pressures up to 93 bar. The phase behavior of the [bmim][PF$_6$]−CO$_2$ binary system is illustrated in Figure 3 where the mole fraction of CO$_2$ in the IL-rich phase is plotted as a function of pressure. The solubility of CO$_2$ in the IL increased dramatically with increasing pressure, reaching 0.72 mole fraction CO$_2$ at 40 °C and 93 bar. Temperature is known to have a dramatic affect on the solubility of a gas in a liquid phase. Generally one may expect an increase in temperature to yield a decrease in gas solubility. As expected, the solubility of CO$_2$ in the IL-rich liquid phase decreased with an increase in temperature, as shown in Figure 3, but the temperature dependence is quite small over this temperature and pressure range. As a result, we do not report the enthalpy and entropy of dissolution since the uncertainties in these quantities would be too large to yield meaningful results. The large degree of CO$_2$ solubility in the IL decreased the viscosity of the liquid phase, as observed by the reduced drag on the stirring magnet.
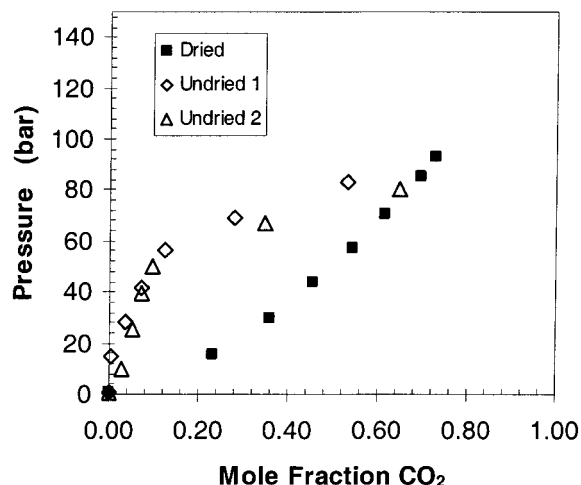
Figure 4. [bmim][PF$_6$]−CO$_2$ liquid phase compositions for dried vs wet ionic liquid samples at 40 °C.

The solubility data of CO$_2$ in [bmim][PF$_6$] shown in Figure 3 is dramatically different than previously reported by our group.[8] Although our preliminary experiments indicated high solubility of CO$_2$ in [bmim][PF$_6$] at higher pressures, the solubility at lower pressures appeared to be relatively low. The discrepancy can be attributed to the small amount of water dissolved in the ionic liquid; the previous IL sample was saturated with water while the current samples were dried to approximately 0.15 wt % water. Measurements in our laboratory indicate that [bmim][PF$_6$] saturated with water at 22 °C contains as much as 2.3 wt % water. Drying of IL samples prior to use is crucial as a small amount of water in the IL has a dramatic effect on the phase behavior with CO$_2$. A direct comparison of the phase behavior of the two samples with CO$_2$ is shown in Figure 4. The difference in CO$_2$ solubility at 57 bar, for example, is dramatic: 0.54 mole fraction CO$_2$ for the dried IL sample compared to 0.13 for the water-saturated sample. The difference in phase behavior is not surprising due to the CO$_2$-phobic nature of water as seen by the very low mutual solubilities of water and CO$_2$, even at high pressures.[13] Another consideration is the formation of carbonic acid from the reaction of CO$_2$ with water that can result in a reduction of the aqueous phase pH to as little as 2.80.[14] Thus, the water impurity in the IL, through chemical and physical mechanisms, is the likely culprit responsible for the low CO$_2$ solubilities in the water-saturated IL-rich phase reported in our earlier publication.[8]

The majority of this work focuses on the IL-rich phase composition of each ionic liquid−CO$_2$ system. Also of interest is the concentration of the ionic liquid in the CO$_2$-rich phase. The solubility of [bmim][PF$_6$] in CO$_2$, carried out on the dynamic apparatus, was determined at 40 °C and 137.9 bar by flowing 0.5866 mol of CO$_2$ through a cartridge loaded with [bmim][PF$_6$]. UV−vis analysis of the collection flask yielded no appreciable [bmim][PF$_6$] absorption peak, indicating a [bmim][PF$_6$] solubility of less than 5×10^{-7} in the CO$_2$-rich phase. The lack of ionic liquid solubility in the CO$_2$ phase is very important in using supercritical CO$_2$ for the extraction of a solute from an ionic liquid. Since no measurable ionic liquid dissolves in the CO$_2$-rich phase, a solute dissolved in an IL can be recovered in pure form without any IL contamination.

Measurement of the compositions for both the IL-rich and CO$_2$-rich phases gives a general idea of ionic liquid−CO$_2$ phase behavior; however, we are interested in the full phase diagram. In particular, does the phase envelope close with an increase in pressure, as is typical of organic liquid−CO$_2$ systems?[10] Due
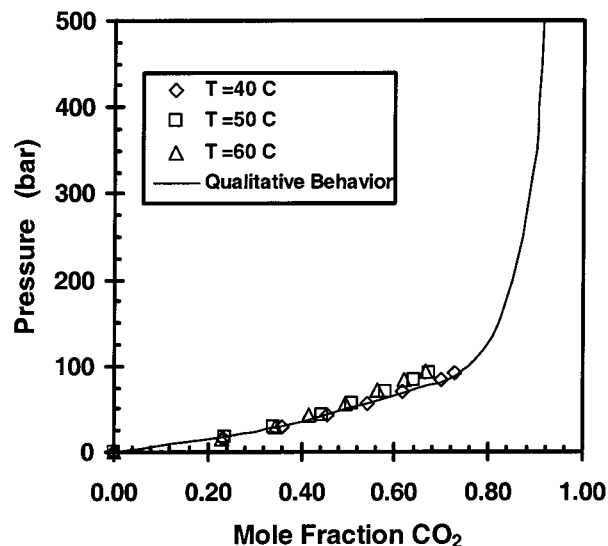

Figure 5. Qualitative phase behavior of the [bmim][PF$_6$]−CO$_2$ system.

TABLE 1: Ultrahigh-Pressure [bmim][PF$_6$]−CO$_2$ Data

T (°C)	P (bar)	wt % [bmim][PF$_6$]	mol % [bmim][PF$_6$]	observation
21.0	2509.2	18.3	3.1	two phases
40.0	3102.8	18.3	3.1	two phases
98.8	1391.4	32.5	6.9	two phases

to the pressure limitation of the static apparatus, phase measurements under higher pressures were performed in a variable volume view cell. Three cloud point measurements of 1.31, 4.92, and 7.15 mol % IL mixtures (with the balance being CO$_2$) were conducted at 400 bar and 25 °C, indicating two-phase immiscibility regions for all samples.[8]

As a complement to the work reported here, McHugh and co-workers have taken [bmim][PF$_6$]−CO$_2$ mixtures to even higher pressures, up to 3100 bar, and found that two distinct phases exist at all conditions tested. As shown in Table 1, phase immiscibility persists even at elevated temperatures.[15] These experiments were performed with the water-saturated sample used in our previous investigation,[8] but we anticipate qualitatively similar behavior at high pressures with dried samples, as well. Based on these experiments, Figure 5 gives a qualitative phase diagram of the [bmim][PF$_6$]−CO$_2$ system over a wide pressure range. This type of phase behavior, with a large immiscibility gap even at extremely high pressures, is very unusual for a liquid−CO$_2$ system. A system in which large amounts of CO$_2$ dissolve in the liquid phase at low pressure generally exhibits a simple two-phase envelope with a mixture critical point at moderate pressures. The formation of a three-phase liquid−liquid−vapor mixture is also common; however, mixtures of compounds that are liquid at ambient conditions with CO$_2$ are usually single-phase, across the entire composition range, at pressures greater than a couple hundred bar. One exception is the H$_2$O−CO$_2$ system, which exhibits very small mutual solubilities (small solubility of H$_2$O in the CO$_2$-rich phase and small solubility of the CO$_2$ in the aqueous phase). Thus, CO$_2$−ionic liquid phase behavior is dramatically different than any normal organic liquid−CO$_2$ phase behavior and is, therefore, important for both theoretical and practical reasons. The mixture molar volumes were also measured, as shown in Figures 7 and 8, and these are discussed in detail below.

[C$_8$mim][PF$_6$], [C$_8$mim][BF$_4$], [bmim][NO$_3$], [N-bupy]-[BF$_4$], and [emim][EtSO$_4$]−CO$_2$. To further explore the unusual IL−CO$_2$ phase behavior, the solubility of CO$_2$ was

TABLE 2: Ionic Liquid–CO_2 Solubility (X_{CO_2}) and Liquid Molar Volumes (mL/mol) at 40, 50, and 60 °C and Elevated Pressures

	$T = 40$ °C			$T = 50$ °C			$T = 60$ °C		
ionic liquid	P (bar)	X_{CO_2}	mL/mol	P (bar)	X_{CO_2}	mL/mol	P (bar)	X_{CO_2}	mL/mol
[bmim][PF$_6$]	0.97	0.000	216.2	0.97	0.000	215.6	0.97	0.000	215.6
	15.17	0.231	172.7	17.38	0.236	171.2	15.79	0.228	171.3
	29.52	0.360	142.3	30.07	0.339	152.4	29.10	0.343	150.0
	43.58	0.455	131.6	42.89	0.444	131.7	42.27	0.416	137.0
	57.09	0.543	114.2	57.00	0.510	119.2	56.54	0.495	121.7
	70.33	0.616	98.3	70.19	0.581	104.5	71.43	0.564	107.9
	84.95	0.698	76.1	84.19	0.640	92.0	83.77	0.620	95.5
	95.67	0.729	71.2	92.46	0.675	83.9	93.01	0.667	84.5
[C$_8$mim][PF$_6$]	0.97	0.000	280.4	0.97	0.000	280.4	0.98	0.000	290.9
	17.93	0.234	223.2	16.00	0.223	226.3	17.38	0.248	225.0
	29.51	0.353	195.8	29.03	0.355	193.2	30.06	0.350	199.9
	42.06	0.452	173.3	44.27	0.441	172.1	43.51	0.450	173.8
	56.54	0.542	151.2	56.82	0.514	157.8	56.89	0.534	151.1
	70.33	0.628	126.7	70.54	0.584	140.0	71.30	0.603	131.9
	83.98	0.715	100.3	83.98	0.660	116.9	84.60	0.682	108.1
	92.67	0.755	80.2	92.67	0.705	103.0	92.88	0.726	94.8
[bmim][NO$_3$]	0.97	0.00	182.0	0.97	0.00	182.1	0.99	0.00	182.5
	15.47	0.196	149.1	17.12	0.169	154.1	18.37	0.183	151.9
	29.05	0.276	136.6	30.08	0.263	139.0	29.26	0.236	143.3
	42.63	0.342	126.3	42.77	0.336	127.6	44.15	0.314	131.0
	56.70	0.397	117.8	57.39	0.388	120.6	56.01	0.369	122.6
	71.18	0.449	109.5	70.42	0.446	109.1	70.77	0.425	113.5
	83.72	0.497	101.6	84.41	0.498	100.6	84.35	0.480	103.7
	92.00	0.513	99.2	92.62	0.530	95.0	93.17	0.522	95.9
[C$_8$mim][BF$_4$]	0.97	0.000	267.1	0.99	0.000	266.6	0.97	0.000	266.0
	17.26	0.197	221.4	15.61	0.191	221.0	15.61	0.160	230.6
	28.85	0.319	193.7	28.78	0.297	196.6	28.43	0.292	200.5
	44.15	0.417	170.9	43.33	0.398	173.4	43.46	0.373	182.8
	56.70	0.507	149.7	57.18	0.489	152.8	56.15	0.454	164.1
	70.49	0.589	129.2	70.42	0.551	138.2	70.49	0.523	143.1
	83.73	0.658	110.6	83.73	0.627	117.8	84.14	0.605	123.8
	92.90	0.708	96.9	92.28	0.671	106.1	93.73	0.651	111.5
[*N*-bupy][BF$_4$]	0.97	0.000	189.5	1.00	0.000	189.5	1.00	0.000	190.1
	15.47	0.144	166.5	16.57	0.142	165.5	18.65	0.166	161.3
	28.57	0.243	151.1	32.36	0.250	148.6	28.99	0.231	152.7
	43.05	0.331	136.9	41.95	0.306	141.0	42.85	0.298	141.8
	56.43	0.399	127.1	56.98	0.392	126.5	56.71	0.372	130.1
	70.91	0.470	114.8	71.66	0.466	112.9	70.08	0.440	117.9
	83.80	0.533	103.6	83.87	0.532	101.4	84.90	0.511	104.6
	91.59	0.579	94.0	92.35	0.581	92.2	95.80	0.549	98.1
[emim][EtSO$_4$]	0.97	0.000	185.4	0.97	0.000	185.4	0.97	0.000	186.5
	16.43	0.100	168.6	16.22	0.103	168.1	14.36	0.118	166.3
	28.08	0.146	161.8	28.84	0.170	157.3	28.77	0.186	155.1
	42.49	0.249	145.3	42.49	0.223	148.4	44.07	0.263	141.9
	56.48	0.307	137.5	56.07	0.282	141.8	56.48	0.319	133.3
	70.20	0.361	129.5	70.34	0.328	134.9	70.00	0.383	122.6
	84.06	0.401	123.8	83.65	0.384	126.1	83.72	0.433	114.4
	92.68	0.423	121.0	94.27	0.403	124.6	94.61	0.457	111.1

measured at 40, 50, and 60 °C and pressures up to 95 bar in five additional ILs: [C$_8$mim][PF$_6$], [C$_8$mim][BF$_4$], [bmim]-[NO$_3$], [*N*-bupy][BF$_4$], and [emim][EtSO$_4$].

Phase Behavior. A comparison of the liquid phase compositions of the various IL–CO_2 systems at 40 °C is shown in Figure 6. A summary of all the ionic liquid–CO_2 solubility data at 40, 50, and 60 °C is given in Table 2 where X_{CO_2} is the mole fraction of CO_2 in the liquid phase. The solubility of CO_2 in the IL-rich liquid phase was greatest for the ILs with fluorinated anions and followed the general trend of [bmim][PF$_6$]/[C$_8$mim][PF$_6$] > [C$_8$mim][BF$_4$] > [*N*-bupy][BF$_4$] > [bmim][NO$_3$] > [emim]-[EtSO$_4$].

In particular, the solubility of CO_2 is the greatest in the ILs with the PF$_6^-$ anion, with [C$_8$mim][PF$_6$] and [bmim][PF$_6$] giving nearly identical results. The solubility of CO_2 in [C$_8$mim][BF$_4$] is approximately 10% less than in [bmim][PF$_6$] and [C$_8$mim]-[PF$_6$] but 20% greater than in [*N*-bupy][BF$_4$]. The isotherms for [*N*-bupy][BF$_4$] are shaped somewhat differently than those

of the imidazolium-based salts. Thus, isotherms for [*N*-bupy]-[BF$_4$] and [bmim][NO$_3$] cross at 55 bar, with CO_2 solubility slightly higher in [bmim][NO$_3$] at lower pressures and higher in [*N*-bupy][BF$_4$] at high pressures. [bmim][NO$_3$] dissolved less CO_2 than the other two [bmim] salts. The IL that exhibited the lowest solubility of CO_2 in the liquid phase was [emim][EtSO$_4$].

The solubility of CO_2 in all of the ILs increases dramatically with increasing pressure but the exact amount dissolved in the liquid phases varies significantly. For instance, at 70 bar the solubility of CO_2 in [emim][EtSO$_4$] is just 0.36 mole fraction, while it is 0.63 mole fraction in [C$_8$mim][PF$_6$] at the same pressure. Despite these differences, the overall phase behavior of all the IL compounds with CO_2 is really quite similar to that of [bmim][PF$_6$]. Like the [bmim][PF$_6$]–CO_2 system, the solubility of CO_2 in the IL-rich phase changed only slightly with temperature for all of the ILs tested. From this we expect the qualitative phase diagram shown in Figure 5 to be representative of most of the imidazolium and pyridinium salts.

High-Pressure Phase Behavior of CO₂/Ionic Liquids

J. Phys. Chem. B, Vol. 105, No. 12, 2001 **2441**

TABLE 3: Ionic Liquid Densities and Molar Volumes at Ambient Pressure

ionic liquid	density (g/mL)			molar volume (mL/mol)		
	$T = 40$ °C	$T = 50$ °C	$T = 60$ °C	$T = 40$ °C	$T = 50$ °C	$T = 60$ °C
[bmim][PF$_6$]	1.346	1.337	1.330	211.1	212.6	213.7
[C$_8$mim][PF$_6$]	1.211	1.204	1.197	281.0	282.6	284.3
[bmim][NO$_3$]	1.149	1.143	1.136	175.1	176.1	177.1
[C$_8$mim][BF$_4$]	1.080	1.073	1.066	261.2	263.0	264.7
[*N*-bupy][BF$_4$]	1.203	1.197	1.190	185.4	186.3	187.4
[emim][EtSO$_4$]	1.225	1.218	1.213	187.3	188.2	189.1
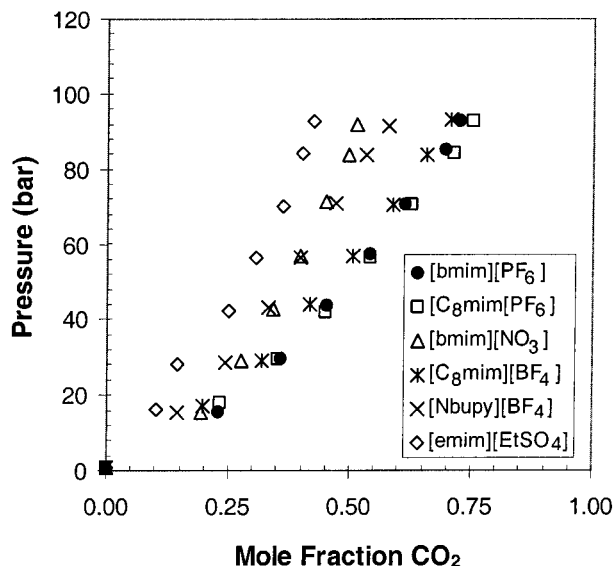
Figure 6. Liquid phase compositions of six ionic liquid−CO₂ mixtures (see text) at 40 °C.

Moreover, this suggests that the successful extraction of solutes from ILs demonstrated with [bmim][PF$_6$][8] is likely to be a general phenomenon; i.e., CO₂ should be able to extract dissolved solutes from any of these ILs too.

Pure Component and Mixture Molar Volumes. The densities of the ILs, measured with a pycnometer at ambient pressure, are given in Table 3. The expected trend of decrease in IL density with an increase in temperature was observed. However, the largest difference in density change over the temperature range was a slight 1.3% for [C$_8$mim][BF$_4$]. A significant difference is observed between the molar volumes of the [PF$_6$] ionic liquids. The C$_8$ chain has a considerably larger molar volume than the C$_4$ chain. From this we can conclude that the length of the alkyl chain has a dramatic effect on the free volume within the liquid. In fact, the two C$_8$ compounds have the largest molar volumes out of all the ionic liquids tested. The size of the anion also has an effect on the molar volume: smaller anions yield smaller molar volumes. For example, the molar volume of [bmim][PF$_6$] is markedly larger than that of [bmim][NO$_3$] owing to the bulkier [PF$_6$] anion. Liquid molar volumes were also calculated at ambient pressure based on measurements from the static apparatus and were within 3% of the pycnometer values.

The most interesting physical chemistry of the ILs is the volumetric behavior of the mixtures with CO₂. The mixture molar volumes for all six ILs with CO₂ were measured at 40, 50, and 60 °C and pressures to 95 bar. An interesting feature of these binary mixtures is that the volume of the IL loaded in the high-pressure cell barely increased even when CO₂ solubility in the liquid phase reached 75.5 mole % CO₂. Figures 7 and 8 represent this phenomenon by the dramatic decrease in mixture molar volumes. Liquid molar volumes for the CO₂−[bmim]-[PF$_6$] system at 40, 50, and 60 °C are shown in Figure 7 and,
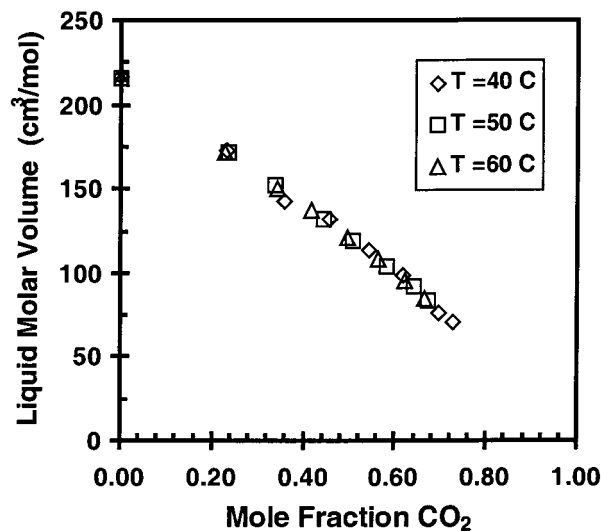
Figure 7. Liquid molar volumes of [bmim][PF$_6$] as a function of CO₂ composition at 40, 50, and 60 °C.
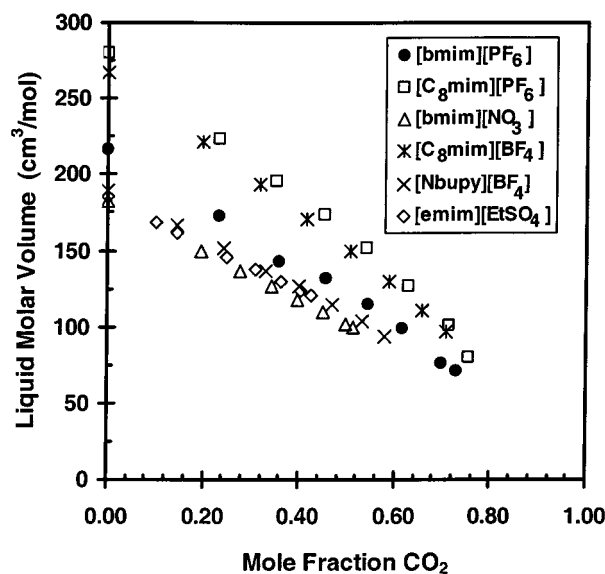
Figure 8. Liquid molar volumes of six different ionic liquids (see text) as a function of CO₂ composition at 40 °C.

similar to the phase behavior, exhibit a weak temperature dependence.

Dilation of a liquid is a well-known phenomenon resulting from the dissolution of a gas into a normal organic liquid phase. Ionic liquids show only slight dilations in volume with CO₂ dissolution. The liquid phase composition of 0.69 mole fraction CO₂ for [bmim][PF$_6$] produces a mere 18% volume increase over the pure IL, resulting in the very small mixture molar volumes in Figure 7. This behavior is very different than normal organic−CO₂ mixtures. For example, a liquid phase composition of 0.740 mole fraction CO₂, for a toluene−CO₂ system at 40 °C and 70 bar, will give a 134% increase in volume of the liquid

phase. Research has shown that all normal liquids exhibit the same substantial percent expansion for a given CO_2 solubility. In fact, the dissolution of CO_2 in liquids to expand them and reduce their solvent strength is well-known and is the basis of the gas anti-solvent (GAS) process to precipitate solutes from liquids.[16] Clearly ionic liquids do not follow this trend. The unusual biphasic behavior of CO_2–IL systems involves not only the presence of a large immiscibility region but also the dilation of the IL-rich phase, upon dissolution of large amounts of CO_2, which is very small when compared to that of traditional organic–CO_2 systems.

Figure 8 is a comparison of the liquid molar volumes for all the ionic liquid–CO_2 mixtures at 40 °C. Molar volumes for each temperature are given in Table 2. The same trend was observed for each isotherm and is given in order of largest molar volume: $[C_8mim][PF_6] > [C_8mim][BF_4] > [bmim][PF_6] > [emim][EtSO_4] > [N\text{-}bupy][BF_4] > [bmim][NO_3]$.

The molar volumes of all the IL–CO_2 mixtures decrease dramatically with increasing CO_2 solubility. This simply reflects the lack of significant expansion of any of the liquids when CO_2 is dissolved in them. An interesting question that is not answered by this study is whether the solvent power of the IL decreases with the addition of CO_2, as is typical of liquid–CO_2 mixtures. Since the density remains high, will the solubility of, for instance, solid solutes in the IL decrease or increase with the addition of CO_2?

Discussion

Combination of the phase behavior and liquid molar volume data provide an insight into the unique phase behavior of CO_2–IL mixtures (Figure 5). The lack of any appreciable dissolution of ionic liquid in the CO_2 phase can be attributed to the extremely low vapor pressures of ILs and the inability of CO_2 to adequately solvate ions in the gaseous phase. Additional measurements in our laboratory indicate a slight evaporation of $[C_8mim][PF_6]$ at 75 °C and 10^{-9} bar, suggesting that an upper limit on the vapor pressure of this ionic liquid is on the order of 10^{-9} bar at 75 °C. Of course, this slight evaporation could be due to the loss of any decomposition products, rather than a reflection of the true vapor pressure of the molten salt.

While large amounts of CO_2 dissolve into the IL phase, the normal volume expansion of the liquid is not observed. We hypothesize that this is due to the strong Coulombic forces between the ions such that separation of those ions would result in too large of a thermodynamic penalty. Increasing the pressure will cause the essentially pure CO_2 phase to increase in density, but since the liquid phase does not expand the two phases will never become identical; that is, a mixture critical point will never be reached. Because of this unique phenomenon, IL–CO_2 systems remain two-phase even at extremely high pressure, as confirmed by the ultrahigh-pressure cloud point measurements of McHugh and co-workers[15] and shown schematically in Figure 5.

The differences between IL–CO_2 phase behavior and that of nonionic organics with CO_2 is further emphasized by comparison with the phase and volumetric behavior of 1-methylimidazole and CO_2. 1-Methylimidazole is a reactant in the synthesis of imidazolium-based ionic liquids. Figures 9 and 10 compare the phase behavior and liquid molar volumes, as a function of CO_2 mole fraction, of 1-methylimidazole–CO_2 and $[bmim][PF_6]$–CO_2. At pressures below 80 bar the CO_2 solubility in 1-methylimidazole is less than in $[bmim][PF_6]$. For example, at 50 bar the CO_2 solubility in 1-methylimidazole is 0.32 mole fraction, while it is 0.50 mole fraction in $[bmim][PF_6]$ at the
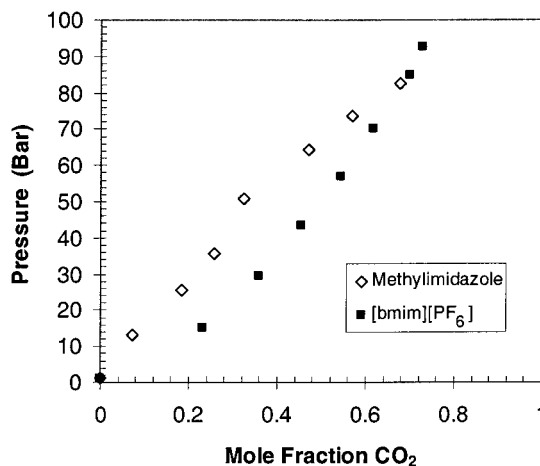

Figure 9. Comparison of liquid phase compositions of the [bmim]-$[PF_6]$–CO_2 and 1-methylimidazole–CO_2 systems at 40 °C.
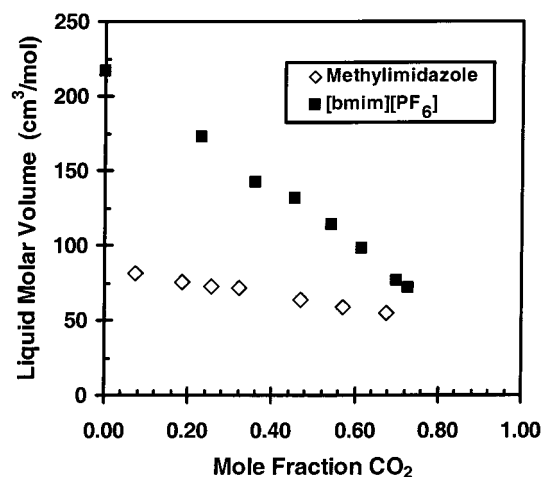

Figure 10. Liquid molar volumes of 1-methylimidazole as a function of CO_2 composition at 40 °C.

same conditions. However, at 83 bar the solubility of CO_2 in both liquids is approximately 0.68 mole fraction. Large differences exist not only in the amount of CO_2 dissolved in the liquid phase but also in the shape of the liquid phase composition curve. The 1-methylimidazole–CO_2 curve is concave, which is typical of most liquid/CO_2 systems. It is an indication of the closing of the two-phase envelope at just slightly higher pressures, implying the presence of a mixture critical point above which exists a single-phase region. By contrast, the IL–CO_2 systems are convex, indicating the approach to a large two-phase region that extends to very high pressures. This behavior is shown clearly in Figure 9 for the $[bmim][PF_6]$–CO_2 system, which remains two-phase even under pressures of 3100 bar. Comparison of the 1-methylimidazole–CO_2 and $[bmim][PF_6]$–CO_2 volumetric behavior emphasizes the dramatic differences between ionic liquids and normal organic liquids. $[bmim][PF_6]$ expands only 18%, even when the liquid phase contains 0.69 mole fraction CO_2 (which occurs at 85 bar). Conversely, 1-methylimidazole exhibits a volume increase of 103% at the same conditions.

Thus, it is clear that the phase behavior of CO_2 with ionic liquids is dramatically different than with normal organic liquids. Although CO_2 solubility is quite high, the mixtures never become single-phase. The liquid phase does not expand, despite the introduction of large amounts of CO_2 into the liquid. Finally, the solubility of the IL in the CO_2-rich phase is immeasurably small. Nonetheless, there are some differences in the phase

behavior of CO_2 with the various ionic liquids studied, and these differences are discussed below.

The effect of the anion of the IL on the phase behavior can be explored by comparing two pairs of ILs that share common cations: [C₈mim][PF₆]−[C₈mim][BF₄] and [bmim][PF₆]−[bmim][NO₃]. Changing the anion from [PF₆] to [BF₄] in the [C₈mim] salts results in an approximately 8% decrease in CO_2 solubility at 40 °C over the range of pressures studied. The liquid molar volumes of these two salts, as well as their mixtures with CO_2, are almost identical: [C₈mim][BF₄] is just about 3% less than [C₈mim][PF₆]. The differences between [bmim][PF₆] and [bmim][NO₃] are more substantial. The solubility of CO_2 in [bmim][NO₃] is about 25% less than in [bmim][PF₆]. However, the molar volumes of [bmim][NO₃] and its mixtures with CO_2 are also substantially smaller (about 15%) than those of [bmim]-[PF₆].

Using ATR−IR spectroscopy, Kazarian et al.[17] have recently shown that CO_2 forms weak Lewis acid−base complexes with the anions in [bmim][PF₆] and [bmim][BF₄]. Moreover, the interaction is stronger with [bmim][BF₄], although they note that the solubility of CO_2 in [bmim][BF₄] is less than in [bmim]-[PF₆]. This is consistent with the results presented here, which show higher CO_2 solubility in [C₈mim][PF₆] than in [C₈mim]-[BF₄]. Thus, we conclude that the relatively high CO_2 solubility in the ILs with the fluorinated anions is at least in part due to a weak Lewis acid−base complex formation but that additional factors, such as free volume, are important in determining the ultimate CO_2 solubility.

The role the IL cation has on the phase behavior with CO_2 can be explored through the comparison of the [C₈mim][PF₆]−[bmim][PF₆] and the [C₈mim][BF₄]−[*N*-bupy][BF₄] systems. In the first case, increasing the length of the alkyl chain on the imidazolium ring from C₄ to C₈ has very little effect on the CO_2 solubility, even though the molar volume of [C₈mim][PF₆] is significantly greater. CO_2 solubility in [C₈mim][BF₄] is about 20% greater than in [*N*-bupy][BF₄].

The IR spectroscopy studies of CO_2 in [bmim][PF₆] and [bmim][BF₄] mentioned above[17] found no evidence of specific interactions of CO_2 with the cation. Thus, we do not attribute the high solubility of CO_2 in ILs to interaction with the acidic hydrogen in the 2-position of the imidazolium cation or with the nitrogens in the imidazolium or pyridinium rings. Moreover, the solubility data do not suggest any specific interactions with the cation. For instance, if there were reversible complexation of CO_2 with the nitrogens, then one might expect the solubility of CO_2 in an ionic liquid containing one nitrogen, the pyridinium ring of [*N*-bupy][BF₄], for example, to be considerably less than in an imidazolium-based IL. As clearly seen in Figure 6, this is not the case. Thus, we conclude that the high solubility of CO_2 in ILs is probably not due to specific chemical interactions between CO_2 and the cation.

As mentioned repeatedly above, there appears to be a rough correlation between the liquid molar volume of the IL and CO_2 solubility. The liquid molar volume, while not quantitative, gives a good indication of "free volume" or "void space" available in the IL phase. For all of the ILs investigated, all of which apparently have strong attractions with CO_2, there is generally greater solubility in the ILs with larger molar volumes. In fact, the almost linear CO_2 solubility as a function of pressure (Figure 6) suggests a space-filling mechanism. Once the void space within the IL is saturated, even under very high pressures, no more CO_2 can dissolve into the ionic liquid. This would be consistent with the observed immiscibility, even at high pressures, as shown schematically in Figure 5. However, further investigations are needed to determine if free volume plays any more than a secondary role in determining CO_2 solubility in ionic liquids.

The combination of ILs and CO_2 exhibits a unique type of phase behavior. The dominating factor in this phase behavior is the fact that the liquid does not significantly expand, even with a large quantity of dissolved CO_2, due to strong Coulombic forces associated with the ionic nature of ILs. The variation of phase behavior between the IL−CO_2 binary mixtures appears to be a function of the strength of general physical interactions with both the cation and the anion. In addition, there appears to be some correlation of CO_2 solubility with liquid molar volume. These factors combine to determine the unusual phase behavior of IL−CO_2 mixtures, which provides a unique opportunity to use supercritical CO_2 in the development of product recovery techniques from ionic liquids.

Conclusions

The applicability of supercritical CO_2 for extraction of solutes from an ionic liquid relies heavily on the phase behavior of the binary IL−CO_2 system. CO_2 dissolution in the IL-rich phase not only is necessary for contact with the desired solute but also decreases the viscosity of the IL. We have shown that CO_2 readily dissolves in the liquid phase of all the ILs tested, while the IL remains insoluble in the CO_2 vapor phase. Although supercritical CO_2 extraction of solutes from an IL has been shown to be successful, processes employing CO_2 and ILs cannot be developed without full understanding of the underlying physical interactions between the two species. In an effort to gain a deeper insight into the unusual phase behavior of ionic liquids with CO_2, the substituents on the cation and the nature of the IL anion were varied. CO_2 solubility depends on the nature of both these species. Moreover, there appears to be some correlation of the CO_2 solubility with liquid molar volume. Thus, by varying the substituents on the cation and nature of the anion, one should be able to design ionic liquids to achieve the desired phase behavior characteristics.

References and Notes

(1) Seddon, K. R. *Kinetics Catal.* **1996**, *37,* 693.
(2) Holbrey, J. D.; Seddon, K. R. *Clean Prod. Process.* **1999**, *1*, 233.
(3) Chauvin, Y.; Olivier-Bourbigou, H. *CHEMTECH* **1995**, *25*, 26.
(4) Wilkes, J. S.; Zaworotko, M. J. *J. Chem. Soc., Chem. Commun.* **1992**, *13, 965.
(5) Welton, T. *Chem. Rev.* **1999**, *99,* 2071.
(6) Visser, A. E.; Swatloski, R. P.; Rogers, R. D. *Green Chem.* **2000**, *2* (1), 1.
(7) Huddleston, J. G.; Willauer, H. D.; Swatloski, R. P.; Visser, A. E.; Rogers, R. D. *Chem. Commun.* **1998**, *16,* 1765.
(8) Blanchard, L. A.; Hancu, D.; Beckman, E. J.; Brennecke, J. F. *Nature* **1999**, *399,* 28.
(9) Blanchard, L. A.; Brennecke, J. F. *Ind. Eng. Chem. Res*. **2001**, *40*, 287.

2444 *J. Phys. Chem. B, Vol. 105, No. 12, 2001*

Blanchard et al.

(10) Dohrn, R.; Brunner, G. *Fluid Phase Equilib.* **1995**, *106* (1−2), 213.

(11) Stradi, B. A.; Kohn, J. P.; Stadtherr, M. A.; Brennecke, J. F. *J. Supercrit. Fluids* **1998**, *12* (2), 109.

(12) Tarantino, D. E.; Kohn, J. P.; Brennecke, J. F. *J. Chem. Eng. Data.* **1994,** *39* (1), 158.

(13) King, M. B.; Mubarak, A.; Kin, J. D.; Bott, T. R. *J. Supercrit. Fluids* **1992,** *5*, 296.

(14) Toews, K. L.; Schroll, R. M.; Wai, C. M.; Smart, N. G. *Anal. Chem.* **1995***, 67 (22)*, 4040.

(15) McHugh, M. A. Personal communication.

(16) de la Fuente Badilla, J. C.; Peters, C. J.; de Swaan Arons, J. *J. Supercrit. Fluids* **2000**, *17,* 13.

(17) Kazarian, S. G.; Briscoe, B. J.; Welton, T. *J. Chem. Soc., Chem. Commun.* **2000**, 2047.